Copper adsorption potentials of MgO(001)

Ye Li and David C. Langreth
Department of Physics and Astronomy, Rutgers University, P.O. Box 849, Piscataway, New Jersey 08855-0849

Mark R. Pederson
Complex System Theory Branch, Code 6691, Naval Research Laboratory, Washington, D.C. 20375-5345
(Received 30 January 1995)

The potentials of a copper atom as functions of position outside the MgO surface were evaluated *ab initio*. These all-electron calculations were carried out with a sufficiently complete localized basis set within the local-density approximation. The MgO(001) surface was simulated by the corresponding surface of finite clusters of various sizes; this procedure was found to give a reasonable approximation to the infinite surface. Potentials were evaluated as functions of distance for the configurations with the copper atom above a surface oxygen atom, a surface magnesium atom, and the hollow site halfway between two oxygen atoms. The deepest potential well was found to be the one for the copper atom above the surface oxygen atom. The mechanism for the bonding between the copper atom and the surface was found to be the interaction between the copper 4*s* state and the oxygen 2*p* band.

I. INTRODUCTION

MgO is a large band gap insulator that crystallizes in the NaCl structure. Its bulk electronic structure has been calculated by several groups,[1–4] and the electronic structure of small clusters of the material has also received attention.[5,6] The simplest and most stable surfaces are the {001} set, which form without reconstruction and with only a small relaxation and rumpling.[8–10] A top view of such a surface is shown in Fig. 1. The properties of such a surface have been the subject of a fair amount of experimental[11–25] and theoretical[4,26–34] study, which has recently been reviewed by Henrich and Cox.[7] The present paper deals with the metallization of such a surface with noble metal atoms. This topic has also been treated experimentally[11–22] and theoretically,[4,31–33] although a unified picture has yet to emerge. In this paper, we treat the case where the adsorbate is Cu, and where the previous theoretical work is even more limited in number, and dealt with the initial stages of metallization. The knowledge of the interaction between Cu and the MgO(001) surface is of great physical importance, because the interaction is related to the activity, selectivity, and the stability of Cu/MgO(001) as a catalyst. The interaction also determines the adhesive energy of the Cu/MgO(001) interface and the growth mode of Cu on this surface.

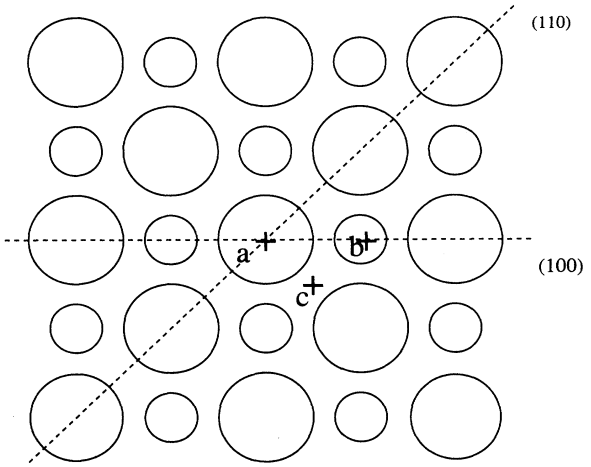

FIG. 1. A "top" view of MgO(001) surface. The figure shows the three configurations for the adsorption potential evaluation. The three sites (*a*, *b*, *c*) above which we put the copper atom are labeled by "+." The (100) and (110) planes are the two planes in which we view the charge density later on.

Specifically, we consider the case of a single Cu atom outside MgO(001). We seek the answers to the following questions. Where is the equilibrium position? How deep is the bonding potential? Where and how high is the saddle point that a Cu atom diffusing on the surface would have to overcome? In short, we are seeking the adiabatic potential felt by the Cu atom as a function of position. Due to the limited computational resources in reality, we picked the three sites, labeled *a*, *b*, and *c*, in Fig. 1, and computed the potentials as functions of distance away from each site perpendicularly to the surface. We expected the absolute minimum to occur over site *a*, with the strongest bonding supplied by the diffuse O^{--} electrons, and the higher three-dimensional saddle point to occur over site *b*, because the Mg^{++} is essentially an inert core, and hence the lower three-dimensional saddle point related to the surface diffusion barrier to occur over the hollow site *c*. For small movements parallel to the surface, the higher three-dimensional saddle point

would be an absolute maximum, while the lower three-dimensional saddle point would be the two-dimensional saddle point providing the intermediate state for surface diffusion. These expectations were confirmed by our calculations, although the strength of the bond between the Cu and the MgO surface was a surprise.

The paper is organized as follows: in Sec. II, we describe the calculational method briefly; in Sec. III, we present our results; in Sec. IV, we discuss our results in the context of other work, both theoretical and experimental; a conclusion is made in Sec. V.

II. METHOD

The calculations are based on the Hohenberg-Kohn-Sham local-density approximation[35] (LDA) with full electron potentials. The total energy of a system of N electrons and M nuclei are evaluated according to

$$E = \frac{1}{2}\sum_{\mu,\nu=1}^{N}{}' \frac{Z_\mu Z_\nu}{|\vec{R}_\mu - \vec{R}_\nu|} + \sum_{i=1}^{N}\langle\psi_i| - \tfrac{1}{2}\nabla^2 + V_{\rm nuc}(\vec{r})|\psi_i\rangle + \frac{1}{2}\int d\vec{r}\int d\vec{r}\,'\frac{\rho(\vec{r})\rho(\vec{r}\,')}{|\vec{r}-\vec{r}\,'|} + \int d\vec{r}\rho(\vec{r})\epsilon_{\rm xc}(\rho(\vec{r}))\,, \quad (1)$$

where $\epsilon_{\rm xc}(\rho)$ is the exchange-correlation energy per unit charge for a uniform electron gas of electronic charge density ρ, neutralized by a uniform positive jellium, and where $V_{\rm nuc}$ is the Coulomb potential from the nuclei, i.e.,

$$V_{\rm nuc}(\vec{r}) = -\sum_{\mu=1}^{M}\frac{Z_\mu}{|\vec{r}-\vec{R}_\mu|}, \quad (2)$$

where $\vec{R}_\mu$ and Z_μ are the position and the charge of the μth nucleus, respectively. The charge density is

$$\rho(\vec{r}) = \sum_{i=1}^{N}|\psi_i(\vec{r})|^2\,, \quad (3)$$

where the label i includes the spin index; the sum on i runs over the N occupied single-particle Kohn-Sham states. The Schrödinger-like equation for these states is obtained from the total energy variationally, yielding

$$[-\tfrac{1}{2}\nabla^2 + V_{\rm eff}(\vec{r})]\psi_i(\vec{r}) = \lambda_i\psi_i(\vec{r})\,, \quad (4)$$

where

$$V_{\rm eff}(\vec{r}) = V_{\rm nuc}(\vec{r}) + \int d\vec{r}\,'\frac{\rho(\vec{r}\,')}{|\vec{r}-\vec{r}\,'|} + \frac{\partial}{\partial\rho}(\rho\epsilon_{\rm xc}(\rho))\bigg|_{\rho=\rho(\vec{r})}. \quad (5)$$

In terms of the eigenvalues λ_i, the total energy E may be expanded using Eq. (4) as

$$E = \frac{1}{2}\sum_{\mu,\nu=1}^{N}{}'\frac{Z_\mu Z_\nu}{|\vec{R}_\mu - \vec{R}_\nu|} + \sum_{i=1}^{N}\lambda_i - \frac{1}{2}\int d\vec{r}\int d\vec{r}\,'\frac{\rho(\vec{r})\rho(\vec{r}\,')}{|\vec{r}-\vec{r}\,'|} - \int d\vec{r}\rho(\vec{r})\,\frac{\partial\epsilon_{\rm xc}(\rho)}{\partial\rho}\bigg|_{\rho=\rho(\vec{r})}. \quad (6)$$

The single-particle eigenfunctions $\psi_i(\vec{r})$ are obtained by expanding them in a finite set of basis functions, diagonalizing the resulting matrix equation, and iterating to self-consistency. These basis functions include a linear combination of atomic orbitals (the radial parts of each expanded in a sum of Gaussians), plus a number of free Gaussians times appropriate angular functions. By making use of the properties of the Gaussians, the "kinetic" part and the nuclear potential part of the single-particle Hamiltonian matrix are evaluated analytically, while the other parts are obtained by numerical integration. The Coulomb potential due to the electron density is calculated analytically at each mesh point. The exchange-correlation potential is in Ceperley-Alder form,[36] parametrized by Perdew-Zunger.[37] The details of the calculational procedure can be found elsewhere.[5,38]

The set of basis functions was constructed according to standard techniques. Fourteen single Gaussians were used for the oxygen atom, sixteen single Gaussians for the magnesium atom and nineteen single Gaussians for the copper atom. Details can be found in the Appendix. The same codes and the magnesium and oxygen basis were also used in our previous surface structure calculations.[8] For a 64-atom MgO cluster of T_d symmetry, we found excellent agreement between the Hellman-Feynman forces and the gradients of energy curves. The copper basis was tested on a Cu-O dimer. Standard superposition error checks (for example, that the addition of an empty Cu basis did not effect the MgO calculations) were made.

III. CALCULATIONS AND RESULTS

We studied configurations with the copper atom above a surface oxygen atom, a surface magnesium atom, and a hollow site equidistant from two nearby surface magnesium atoms and two nearby surface oxygen atoms (sites a, b, and c, respectively, in Fig. 1). For each case, the distance from the copper atom to the surface was varied. At each distance, the total energy was evaluated, and from it was subtracted the total energy of the isolated copper atom and the isolated MgO cluster, thus giving adsorption potentials as functions of distance.

In order to make the calculations feasible, the infinite surface was replaced by an unrelaxed finite cluster. Various cluster sizes were used. We argue, for example, that a $5\times5\times2$ or 50 atom cluster is sufficient to get qualitative and probably quantitative results, for an atom above site a. We give a more detailed analysis of the effect of cluster size later, but for now just state that the Madelung field at the equilibrium Cu site is given accurately to about 3% by our cluster, and at twice this distance is negligible

both for the cluster and for a semi-infinite surface; the work to move a charge between these two points is in error by only 10%. The fact that the potential gets worse for still larger distances is not important because all our calculated points are at smaller distances than this. Although all such Madelung errors can be eliminated by embedding the cluster in a point-ion array,[39] such methods must use arbitrary artificial means, such as restricting the basis set, to prevent electrons from condensing into the attractive potential wells of the point-ion array.

The (001) surface of our cluster consists of just those atoms pictured in Fig. 1. One sees that those atoms involved to any significant degree with the bonding (oxygen atoms which are nearest neighbor and second nearest neighbor to the Cu atom) have the same local environment as they would in a semi-infinite crystal. The clusters involved have the atomic spacing of 4.0 a.u. (2.12 Å), the approximate spacing of the bulk crystal. However, the surface relaxation and rumpling are very small for this surface, as has been well established by the previous work of ours[8,9] and others.[10] The extent of further surface distortion as the adatom approaches is of course unknown, although we will make some relevant estimates based on the calculated forces. However, such readjustment is not expected to have much effect on the well depth in the bound position of the adatom, since we find that most of the binding occurs through a bond with the oxygen directly beneath, so that small changes in the positions of the other atoms relative to it should be unimportant.

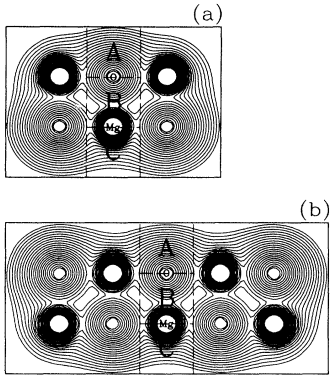

FIG. 2. The total charge densities for the clean MgO clusters plotted in the (100) plane. The contours start from 0.001 a.u. and increase successively by a factor of the square root of 2. Panel (a) is for the $3 \times 3 \times 2$ cluster and (b) is for the $5 \times 5 \times 2$ cluster. We found good match in the central surface region between the two clusters.

A. Clusters without copper

We began with calculations on isolated MgO clusters for three reasons. First, the total energies were needed as reference points for the adsorption potentials. Second, the electronic structure was helpful for the investigation of the nature of the bonding between the copper atom and the clusters. Third, it provided a comparison to the work of others on clean MgO, to confirm our techniques.

1. Charge densities

Figure 2 shows the contour plot of the total charge densities for clusters without the copper atom. Figure 2(a) is for a $3\times3\times2$ cluster, and Fig. 2(b) for a $5\times5\times2$ cluster. The plane of the contour plot is that of (100) as projected in Fig. 1. The charge density for the outermost contour is 0.001 a.u. The density corresponding to each subsequent contour line has a ratio of $\sqrt{2}$ with that of the previous one. By overlaying the two plots, we found that the charge densities in the bulk region (region B in the figure) and surface oxygen region (region A in the figure) were indistinguishable. For the region of surface magnesium, i.e., region C, the two sets of results were distinguishable only at the lowest densities, where for example the distances from the magnesium nucleus at which the density reaches 0.001 a.u. differ by about 5%. The charge densities of the finite clusters were also compared with that of an infinite five-layer slab which was calculated by Li *et al.* with the full-potential linear augmented plane wave (LAPW) method.[4] The densities in the central surface region of the $5\times5\times2$ cluster agree with those in the equivalent regions of the slab surface.

2. Densities of states

The densities of Kohn-Sham states (DOS) were also plotted vs energy eigenvalue (see Fig. 3). The DOS were plotted for neutral clusters of $3\times3\times2$ and $5\times5\times2$ atoms, and a neutral $5\times5\times5$ cluster with 63 O atoms and 62 Mg atoms. In the DOS plot, the set of δ functions was replaced by a set of Gaussians with a finite width of 0.005 Hartree. Generally, we see bands of states similar to the occupied oxygen $2s$ and $2p$ bands and the unoccupied conduction band of the bulk crystal. In addition, one generally sees states that are separated from the bands, which are associated with the fact that our clusters have corners, and we call such states *corner states*. Each corner state was labeled with the letter C or c^* in the figure, depending on whether its respective origin was an O corner or a Mg corner. They were identified by the fact that they have most of their Mulliken populations on the corner atoms.

We calculated the width of the O $2p$ band, the band gap between the O $2p$ band and the conduction band, and the width of the s-p band (from the bottom of the $2s$ band to the top of the $2p$ band). The band gap was from the eigenvalues of the ground state. In the evaluation, the corner states were not included as part of the "bands." The results for the above calculation are tabulated in Table I. Also tabulated are the results from the pseudopotential calculations by Chang and Cohen[1] (in a plane wave basis) and Wang and Holzwarth[3] (in a LAPW basis) for the MgO bulk, the results from the full

TABLE I. Comparison for bandwidths and band gaps of clean MgO. The unit is eV. Width of *s-p* band was measured from the bottom of the O 2*s* band to the top of the O 2*p* band. The corner states were excluded. The values from the work by Wang and Holzwarth and Chang and Cohen were for bulk MgO.

	Width of *s-p*	Width of O 2*p*	Gap between O 2*p* and Cond. bands
3×3×2	16.0	3.5	3.8
5×5×2	16.6	3.8	3.0
5×5×5	16.9	4.4	3.0
Li *et al.* (Ref. 4) slab		4.6	3.5
Li *et al.* (Ref. 4) bulk			5.0
Wang and Holzwarth (Ref. 3)	17.2	4.8	4.4
Chang and Cohen (Ref. 1)	17.1	4.8	4.5
Experiment (Refs. 40 and 41)	20.0	5-6	7.8

potential LAPW calculations[4] by Li, Wu, Freeman, and Fu for the MgO bulk and the MgO five-layer slab, and the experimental values.[40,41] The latter are included to emphasize that even though the Kohn-Sham eigenvalues do not, in general, correspond directly to any experimental quantity even in principle, nevertheless one expects to be able to obtain qualitative information from such calculations. The bandwidths of our finite clusters are in agreement with the bandwidths for the bulk taken from the theoretical work of others and from experiment. The band gaps of our finite clusters are smaller than those of the bulk crystal, at least if everything but corner states are included as part of the "bands." Our cluster calculations are similar in this sense to the recent five-layer slab LAPW calculations,[4] which also found a band gap smaller than that for the bulk. These LDA calculations show 1.5 to 2.0 eV narrowing of the band gap at the (001) surface. The band gap narrowing at this surface has been observed in various experiments,[23–25] and in some other calculations.[27–29] The amount of the narrow-

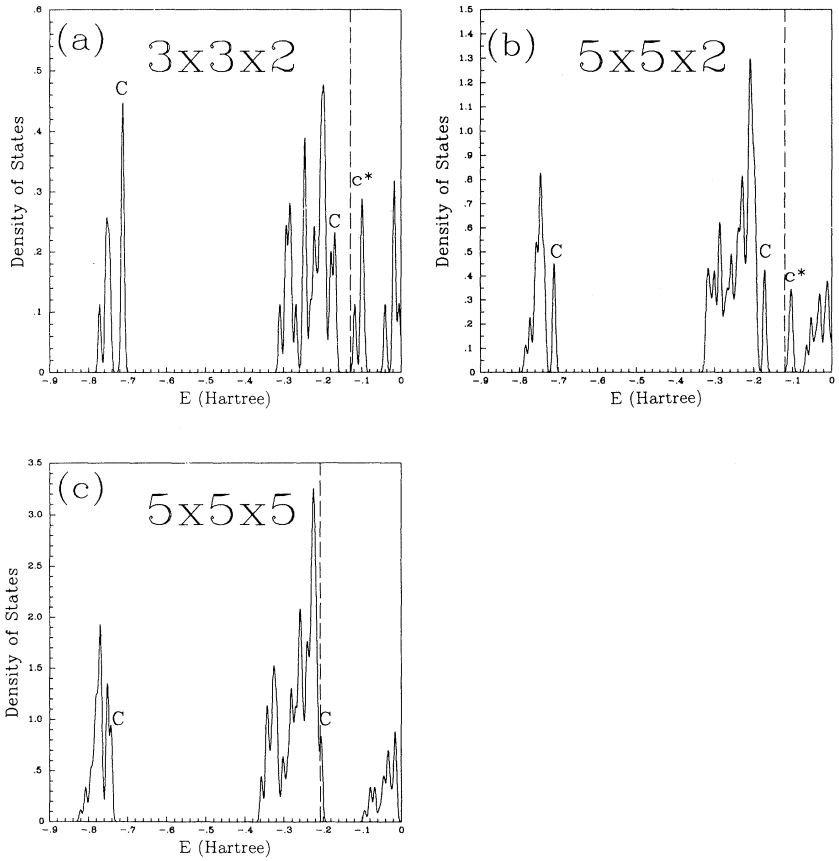

FIG. 3. The densities of states as functions of energy eigenvalues. In the plot, the δ functions are replaced by Gaussian functions of a width of 0.005 Hartree. The unit for the densities is 1000 e/Hartree. The Fermi levels are indicated by dotted lines. These results of (a), (b), (c) are from calculations on $3\times3\times2$, $5\times5\times2$, and $5\times5\times5$ clusters, respectively.

ing from LDA calculations is in good agreement with the experimental results[23–25] and the amount indicated in the self-consistent tight-binding calculation.[29] The extra states in the bulk band gap emerging from the bottom of the (mostly Mg derived) conduction band are presumably surface states resulting from the missing repulsive Kohn-Sham potential v_{eff} near the surface Mg atoms, which is caused by the truncation of the lattice, and which is essentially unscreened near a surface Mg atom because of the lack of mobile Mg electrons. Indeed, surface states were identified in this region in a previous tight-binding calculation,[26] although in that calculation the surface states did not emerge below the absolute band gap. To summarize the comparisons of this paragraph, it is apparent that the DOS of the $5\times5\times2$ and $5\times5\times5$ clusters are very similar to those of the five-layer slab.

3. Surface shifts of core eigenvalues

The surface core shifts in the Kohn-Sham eigenvalues for isolated clusters were also obtained, as shown in Table II. Eigenvalue changes do not represent the best possible LDA calculation of core shifts, which would include the relaxation of the other electrons, but are included here for the purpose of the next subsection as a comparison with the core eigenvalue changes induced by Cu adsorption. The core shift of the surface oxygen is much smaller than that of the surface magnesium. This is because the outer electrons of oxygen atoms can be deformed to screen out partially the electric field on the surface oxygen, and the screening reduces the core shift. The very small core shift of the surface oxygen for the 4×4×4 is different from the very small core shift for the 5×5×5 cluster. In the 4×4×4 cluster, the atom numbers for oxygen and magnesium are the same, but we have one more oxygen atom in this particular 5×5×5 cluster. So, for the 5×5×5 cluster, some corners states are only partially occupied. These partially occupied corners states have most of the distribution on the corner oxygens, but they still have some small fraction of the distribution on the surface oxygens. The electron population at a surface oxygen site of the 5×5×5 cluster is slightly smaller than that of the 4×4×4 cluster, so the surface oxygen core shifts for the two clusters are slightly different as a result. In summary, we have the conclusion that the core shift for the surface oxygen atom is very small, and negligible, while the core shift for the surface magnesium is −0.6 eV.

TABLE II. The surface shifts for oxygen and magnesium 1*s* states. The unit is eV. The 5×5×5 cluster is a neutral cluster with 63 O atoms and 62 Mg atoms.

Cluster	Oxygen	Magnesium
4×4×4	0.12	−0.62
5×5×5	−0.03	−0.61

4. Conclusion

Our results for total charge density and density of Kohn-Sham states showed good agreement with the calculations of others. The agreement for charge densities and the DOS between the finite clusters and the five-layer slab gave reasonable justification for the use of clusters to simulate infinite surfaces.

B. Clusters with a copper atom

In this subsection, the results for adsorption potentials as functions of position are presented, the mechanism for the bonding between the copper atom and the surface is investigated, and the sufficiency of cluster size is confirmed.

1. Adsorption potentials

The calculated copper adsorption potentials as functions of position are shown in Fig. 4. The potentials are zero (by definition) when the copper atom is at infinity. The results are in agreement with what we have anticipated, except for the bonding strength. We assumed that the surface oxygen is the bonding site, and that the hollow site is the site a Cu atom has to go across to migrate. Under this assumption, the bonding strength between the copper atom and the surface is 0.052 hartree (1.42 eV). The equilibrium distance between the copper atom and the surface oxygen atom is 3.70 a.u. (1.89 Å). The diffusion barrier is 0.014 hartree (0.38 eV).

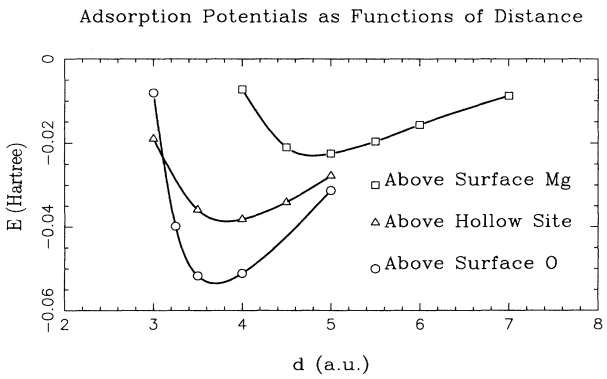

FIG. 4. Adsorption potentials for three configurations. For configurations with the copper atom above the surface oxygen site or above the surface magnesium site, the results are from $5\times5\times2$ MgO clusters. For the configuration with the copper atom above the hollow site, the results are from a $4\times4\times2$ MgO cluster. The potentials are zero when the copper atom is at infinity. The distance d is the distance from the copper atom to the surface.

2. *Charge transfer*

This bonding is surprisingly large given the closed shell MgO and nearly closed shell Cu. We would like to identify the bonding mechanism. First, we investigate the charge transfer between Cu and the MgO cluster, and are able to rule out any significant charge transfer. We do this both by (i) charge integration (here) and (ii) Mulliken analysis (below). Of course due to overlapping charge densities, the notion of charge transfer is not *a priori* well defined in an *ab initio* calculation such as ours. With respect to (i), we make it quantitatively well defined by placing boxes of intuitively chosen sizes around each atom, a procedure which is obviously somewhat arbitrary. Similarly although method (ii) gives results that are well defined, the pitfalls of Mulliken analysis are well known. Nevertheless, we believe that by the combination of the two methods, we establish fairly conclusively that the qualitative notion of charge transfer is not a dominant factor in the bond. In all cases, we work with the $5 \times 5 \times 2$ cluster. Comparisons were made between the case when the copper atom is far away and the case when the copper atom is 4.0 a.u. from the surface.

To obtain the charge transfer from integration, we placed each atom in a box, and watched the change of total charge inside the boxes as the copper atom moved from far away to the surface. The sizes of the boxes were so determined that the charge densities inside the boxes were almost isotropic, and each box was made as large as possible for each atom. The sizes of the boxes were determined from the total charge contour plots (see Fig. 2 and Fig. 5). We placed each oxygen atom in a cubic box of lateral size of 4.8 a.u., each magnesium atom in a cubic box of lateral size of 3.2 a.u. However, we had to place the central surface oxygen and the copper atom into boxes of $4.4 \times 4.8 \times 4.8$ a.u., in order to avoid large overlap between the two boxes when the copper atom gets to the surface. The Mg boxes enclose 99% of Mg $2p$ electrons. The cubic O boxes enclose 97% of the O $2p$ electrons. The box for the central surface oxygen, which is right below the Cu, encloses 96% of O $2p$ electrons. The copper box encloses 52% of the $4s$ electron, and 97% of the $3d$ electrons. If there were any charge transfer, the charge would be to or from the Cu $4s$ state, for it is the outermost state for the Cu atom and it is half occupied. The amount of the oxygen electrons in the copper box due to overlap of the boxes is in the order of 0.03 electrons. So we would be able to observe an appreciable change for the charge inside the copper box if there were any. From charge integration, we observed the following. As the copper atom moves from infinity to the surface, the charge inside the copper box increases by a small amount of 0.11 electrons, while the charge in the central surface oxygen box increases by only 0.06 electrons, and the charge around the side oxygens (those which are the second nearest to the copper atom) increases by 0.11 electrons. The change for the charge around other atoms is smaller than 0.03 electrons each. The net charge change for all the boxes of the magnesium and oxygen atoms is an increase of 0.24 electrons. All these integrated numbers are tabulated in Table III. From the small change inside the copper box, one concludes that there is no significant charge transfer from or to the copper site. The charge increase in the cluster is due to the orbital overlaps between the copper atom and cluster, as more than 0.8 Cu electrons are outside of the copper box.

We conclude this section with a discussion of a type of charge transfer error that can occur in the LDA.[42] The manifestation of it that occurs here results from the fact that at a Cu distance further out than our last calculated point, the Cu $4s$ level drops slightly below the energy of the cluster corner states, although still well above the top of the valence band. This means that the LDA ground state at infinite separation is one in which the Cu atom has fractionally more than 29 electrons, the difference coming from the corner states. Since the eigenvalue difference between the corner states and the Cu $4s$ is only 0.005 hartree, the fractional charge transfer necessary to equalize these eigenvalues is very small; we found that a transfer of 0.02 electron was sufficient. Thus this spurious LDA charge transfer effect is irrelevant on our scale of accuracy, giving an energy error of less than 10^{-4} hartree.

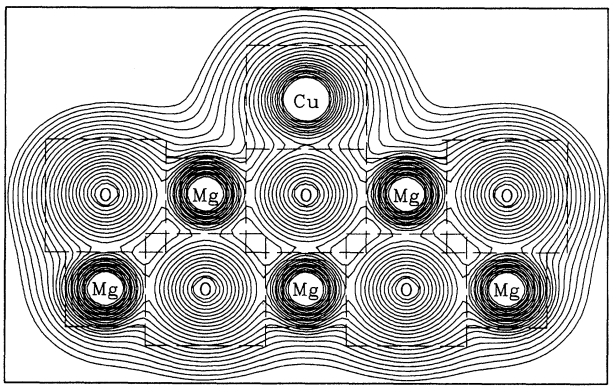

FIG. 5. The total charge densities plotted in the (100) plane for a $5 \times 5 \times 2$ MgO cluster with a copper atom 4.0 a.u. away from the central surface oxygen. The contours start from 0.001 a.u. and increase successively by a factor of $2^{\frac{1}{2}}$. The boxes shown in the figure are the boxes inside which we evaluate the charge later on to investigate charge transfer between the copper atom and the cluster.

TABLE III. Charge transfer as Cu moves to the surface. The side oxygens are the ones second nearest to the copper atom. The amount tabulated for the side oxygens is the total for all the four side oxygens.

	Cu	Central O	Side O	Whole MgO cluster
Charge integration	+0.11	+0.06	+0.11	+0.24
Mulliken analysis	+0.03	+0.29	+0.14	−0.03

TABLE IV. Mulliken distribution of some states of the MgO cluster with Cu. The Cu atom is 4.0 a.u. above the central surface O atom of the 5 × 5 × 2 cluster. The side oxygens are the second nearest to the copper.

States	Weight	Central O	Side O	Cu atom	All MgO sites
Cu $4s^*$	1	0.62	0.07	0.31	0.69
Cu $3d^*$	2	0.09	0.20	0.75	0.25
O $2p^*$	2	1.08	−0.02	0.13	0.87
O $2s^*$	2	0.99	−0.02	0.13	0.87
$\sum_{\text{other}}$ O $2p^*$	2	−0.19	2.08	0.20	10.80
$\sum_{\text{other}}$ O $2s^*$	2	−0.06	0.95	0.15	4.85
Total		4.44	6.45	3.03	35.97

3. *Mulliken analysis*

From the Mulliken analysis, we confirm the lack of charge transfer, and get an indication of the mixing between the copper states and the cluster states, which eventually reveals the bonding mechanism with the help of some charge plots. For reasons to be discussed below, we only have to study the Mulliken distributions of a small number of states. The electronic states are sorted into different group-theoretic representations. Only the states within the same representation can mix with one another. The only important representation is the one which the copper $4s$ state is in. The important spatial states in this representation are one $4s$-like and one $3d$-like state from the copper atom, six states from the oxygen $2s$ band, and twelve states from the oxygen $2p$ band in the 5×5×2 MgO cluster. All the analysis is done within the set of states mentioned above. The representation involved is referred to as the *first* representation.

We counted the Mulliken populations of these first representation states on the surface oxygen sites and on the copper site. When the copper atom moves from infinity to the surface, the Mulliken population on the copper site changes from 3.00 to 3.03, and the population changes from 4.30 to 4.44 on the central surface oxygen site and from 6.16 to 6.45 on the side oxygen sites. (See Table IV and Table V.) The 0.03 increase of the Mulliken population on the copper site, the 0.29 increase on surface oxygen site, and 0.14 increase on the side oxygen sites cannot be quantitatively connected with charge movement, but the fact that they are small, suggests also that the charge transfer is small. Once again, all these are tabulated in Table III, together with the charge integration results.

TABLE V. Mulliken distribution of some states of the isolated MgO cluster and Cu atom.

States	Weight	Central O	Side O	Cu atom	All MgO sites
Cu $4s$	1	0.00	0.00	1.00	0.00
Cu $3d$	2	0.00	0.00	1.00	0.00
$\sum_{\text{all}}$ O $2p$	2	1.24	2.13	0.00	12.00
$\sum_{\text{all}}$ O $2s$	2	0.91	0.95	0.00	6.00
Total		4.30	6.16	3.00	36.00

To get more of an idea of the mixing between the copper states and the cluster states, we observed the change in the composition of certain states. In Table IV, we listed the Mulliken distribution of several important states: Cu $4s^*$, Cu $3d^*$, O $2p^*$, and O $2s^*$; these states are labeled a, b, c, and d, respectively, in Fig. 6 and their charge densities given in panels (a), (b), (c), and (d), respectively, in Fig. 7. The notation here is meant to be transparent: the Cu $4s^*$ and Cu $3d^*$ are what become of the Cu $4s$ and Cu $3d$ states when the Cu is moved close to the surface, while the O $2p^*$ and O $2s^*$ states are the ones that split off from the O $2p$ and O $2s$ bands as the Cu moves close to the surface. The above four states were picked because they have appreciable population on either the Cu site or the central surface oxygen site, or

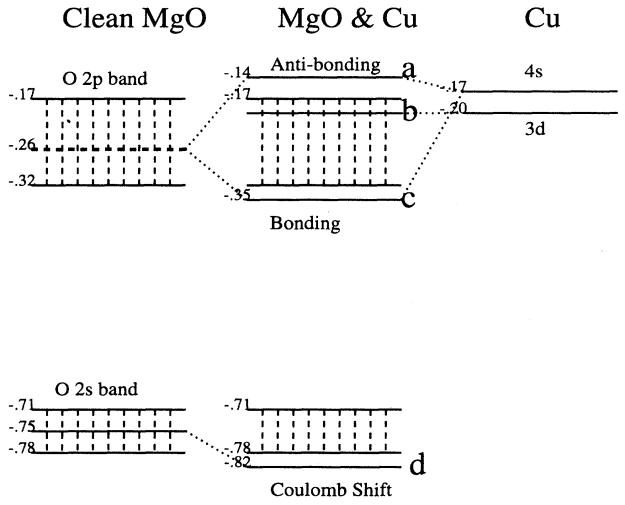

FIG. 6. This figure illustrates the mechanism of the bonding between the copper atom and the MgO surface. The energy labels (in hartree) on each level are those calculated for the 5 × 5 × 2 cluster. The left and the right panels depict the clean MgO cluster and the isolated Cu atom, respectively, while the central panel depicts the level of the joint MgO-Cu cluster with the Cu atom 4.0 a.u. above the central oxygen ion. The squares of the wave functions of the states marked a, b, c, d are shown in Fig. 4.7 (a), 4.7 (b), 4.7 (c), and 4.7 (d), respectively.

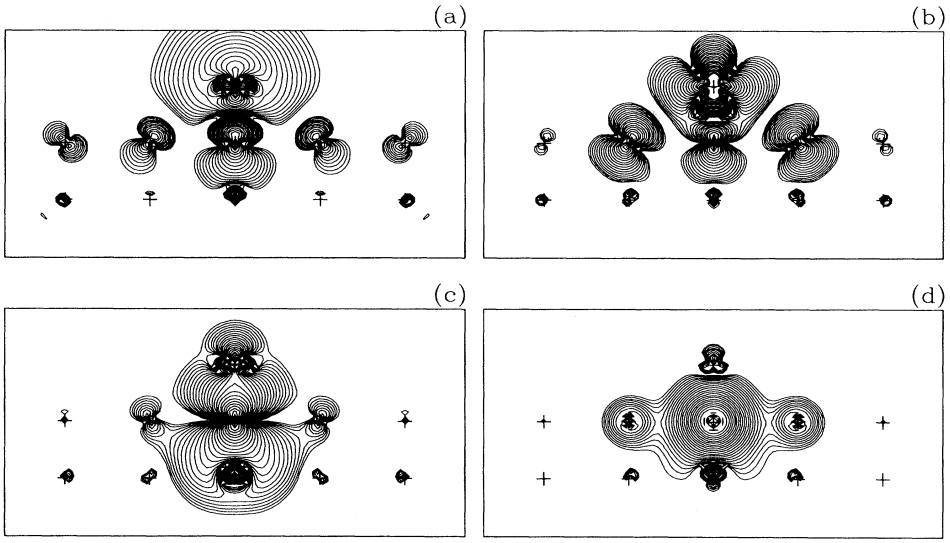

FIG. 7. Charge densities are plotted in the (110) plane for four states of the $5 \times 5 \times 2$ MgO cluster with the copper atom 4.0 a.u. away above the central oxygen. The atomic sites are labeled by "+." Panel (a) is for the state that was Cu $4s$ when the Cu atom is far away. The interaction between the copper atom and the surface oxygen is antibonding. Panel (b) is for the state that was Cu $3d$. For some outer contours, the interaction between the copper atom and the surface oxygen is bonding. For the inner contours, the interaction is antibonding. The net interaction is slightly antibonding. Panel (c) is for the bonding state from the interaction of copper $4s$ state and oxygen $2p$ states. Panel (d) is for the state, which was a O $2s$ state. The mixing between the Cu states and the O $2s$ states is very small and negligible.

on both. We listed the Mulliken distribution on the sites of the copper atom, the surface oxygen right below the Cu atom and the side surface oxygen atoms. The Cu $4s^*$ state has 31% population on the Cu site and 62% on the central surface oxygen site. This suggests that the central surface oxygen atom interacts much more strongly than other atoms with the Cu $4s$ state. The Cu $3d^*$ state has 75% population on the Cu site and 20% on the all four side oxygens (4% on each) and 9% on the central surface oxygen. This Mulliken distribution suggests that the interaction between the copper $3d$ state and the cluster is weaker than that between the Cu $4s$ state and the cluster. The interaction between the Cu $3d$ state with the side oxygens could be comparable to the interaction between the Cu $3d$ state with the central oxygen. The O $2s^*$ and $2p^*$ both show 13% of the population on the Cu site and more than 90% on the central surface oxygen site. Although this suggests that the $2s$ band electrons of the central surface oxygen have about the same importance as those electrons from the $2p$ band for the interaction between the Cu atom and the cluster, we will see later that this is a case where the Mulliken analysis is deceiving, and the $2p$ band electrons play a much greater role.

4. The bonding mechanism

The study of charge plots of the various single-particle states finally reveals the bonding mechanism. The mechanism can be pictured (see Fig. 6) as follows. A strong interaction was found between the copper $4s$ state and the oxygen $2p$ band. The copper $4s$ state and oxygen $2p$ states mix together and form two different states, which we have previously denoted as the Cu $4s^*$ state and the O $2p^*$ state. The charge densities in these states are shown in Fig. 7, panels (a) and (c), respectively. State (a) has a low density minimum in the charge density part way between the O and the Cu indicating a node in the wave function and hence an antibonding interaction. Therefore, one would expect this interaction to raise the energy eigenvalue of this state, and reference to Fig. 6 shows indeed that this state has moved up above the $2p$ band. State (c) on the other hand has a saddle point in its density between the O and Cu, indicating a saddle point in the wave function, and hence a bonding interaction. Therefore, we expect a corresponding eigenvalue lowering, and indeed we see that this state has split off below the $2p$ band. Now state (a) is singly occupied while state (c) is doubly occupied, so that the bonding interaction is predominant. Therefore, in a simple single-particle point of view, this movement of the energies provides the mechanism for bonding.

To make this a little more quantitative, we first ask where the O $2p^*$ state "came from." Analysis of the O $2p$ band density of states projected on the surface oxygen site before and after the Cu is adsorbed shows that it comes rather uniformly from this projected density of states over the whole oxygen $2p$ band. Equivalently, we

can attribute it to having come from a place in an average position in this band, which we have calculated to be −0.26 hartree, as indicated by the dashed line in Fig. 6. Second, some discussion of the Cu d states is in order. First, it is clear from the charge plots that states (a) and (c) have plenty of d admixture, and are certainly not purely s and p. In addition state (b), the Cu $3d^*$ state, shows an interaction with the O $2p$, with the antibonding interaction of the polar lobe of the $3d$ expected to dominate over the bonding interaction of the equatorial bulge in the $3d$. Nevertheless when all effects are put together, the energy eigenvalue of the $3d$ of the isolated Cu is essentially identical to that of the $3d^*$, as indicated in Fig. 6. We can now estimate the change in the eigenvalue sum in the expression for the total energy coming from O valence band states and Cu $3d$ and $4s$ states, that is the change in the second summation in Eq. (6) coming from these states when the Cu is adsorbed. Using the numbers in Fig. 6 gives $2\times(-0.35+0.17)+1\times(-0.14+0.17) = -0.15$ hartree. This is of the same order of magnitude as the actual calculated well depth. To be more precise, however, its magnitude is larger than the actual calculated binding, as expected from the usual double counting arguments; the other terms in Eq. (6) other than the eigenvalue sum will reduce this value.

We have postponed discussing the movement of states in the O $2s$ band region, because different physics is involved, such that the movement here does not appreciably affect the Cu-MgO well depth. State (d), that is the $2s^*$ state of the central oxygen atom, shifts down by an amount of 0.06 hartree (1.6 eV). In contrast to the $2p$ case where the states that are shifted were spread rather uniformly throughout the projected $2p$ density of states, here peaks in the projected density of states around −0.753 hartree disappear when the Cu is adsorbed and the split off state (d) appears at −0.816 hartree. From the charge plot [Fig. 7(d)] of this state, one sees that it has little Cu state admixture. The downward shift of the O $2s$ state is very close to the $1s$ shift, which is 0.05 hartree. From our calculation, we found that Coulomb interaction caused a downward shift of about 0.05 hartree. So, the downshift for the O $2s$ state is due to the change in environment of the charge density. In summary, the $2s$ state of the central oxygen atom does not hybridize with the copper states. The eigenvalue shift is of completely different origin from that of the $2p$ states. Since the $2s$ states are very localized around the oxygen, almost like a core state, the same Coulomb potential that produced the shift, will have a nearly equal and opposite interaction with a corresponding proton in the nucleus, so that the net effect on the well depth will be small.

5. *Cluster size: Effect of bonding atoms in different environments*

The sufficiency of the cluster size is argued in two aspects. First, the difference between the results from clusters of different sizes is discussed; second, in Sec. III B 6 below, the effect of the adsorbed copper atom on all the oxygen $2s$ and $2p$ electrons is studied.

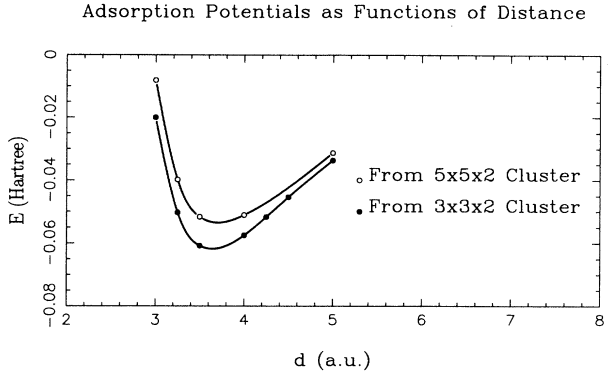

FIG. 8. The potentials are for the configuration with the copper atom above the surface oxygen site. The difference between the results from the two clusters is due to the bonding interaction between the copper atom and the corner oxygen atom in the 3 × 3 × 2 cluster.

Figure 8 shows the results of the adsorption potentials of 5×5×2 and of 3×3×2 for the configuration with the copper atom above the surface oxygen. The two clusters give approximately the same answer for the equilibrium distance between the copper atom and the surface oxygen. However, the bonding strength differs by 0.01 hartree. Although the difference is not qualitative, one has to worry whether it is part of a continuing trend as cluster size increases. The extra bonding for the 3×3×2 comes from the interaction between the copper $3d$ and corner oxygen atoms. Figure 9 shows the contour plot of an electronic state in the 1st representation for the 3×3×2 cluster with a copper atom. One can see that the interaction between the copper $3d$ state and the $2p$ orbitals of the corner atoms is indeed bonding. And the phase difference between the $2p$ orbital of the surface oxygen and the $2p$ orbitals of corner oxygens happens to be so much that the interaction between the copper $3d$ and central surface oxygen $2p$ orbital is also bonding. This kind of interaction happens to the 3×3×2 atom cluster because the local environment of the side oxygens of this cluster is different from their local environment in the 5×5×2 cluster. This kind of interaction is not seen for the 5×5×2 cluster. In all clusters of 5×5×2 and larger, the side oxygens have the same local environment as they would in the infinite surface, so that the change in bonding strength in going to still larger two layer clusters is expected to be much smaller than 0.01 hartree.

6. *Cluster size: Average local energy shift*

Here, we argue that the 5 × 5 × 2 cluster is also thick enough as well as two-dimensionally large enough for this problem. The argument is based on the study of the average local energies of the O $2s$ and $2p$ electrons in the first representation on each oxygen site. We define the average local energies from the Mulliken distribution. Let us take the $2s$ electron on the central surface oxygen atom,

TABLE VI. Copper-induced energy level changes for oxygen electrons. The MgO cluster is a $5 \times 5 \times 2$ cluster. $S1$ is the oxygen right below the Cu atom; $S2$ represents the four oxygens second nearest to the copper atom; $S3$ represents the surface oxygens in the second layer; $E1$ and $E2$ are oxygen sites at the cluster edges in the first layer and second layer, respectively; C is the corner oxygen sites. The changes are those when the copper atom comes from infinity to the position 4.0 away above the central surface oxygen. The core shifts are copper induced $1s$ shifts.

Changes of energy level of O $2s$ electrons						
	$S1$	$S2$	$E1$	C	$S3$	$E2$
ΔE	−0.063	−0.003	−0.003	−0.002	−0.007	−0.003
ΔE_{core}	−0.047	−0.005	−0.002	−0.002	−0.008	−0.002
$\Delta E - \Delta E_{\text{core}}$	−0.011	0.002	−0.001	0.000	0.001	−0.001
Changes of energy level of O $2p$ electrons						
	$S1$	$S2$	$E1$	C	$S3$	$E2$
ΔE	−0.039	−0.002	0.001	−0.002	−0.011	−0.002
ΔE_{core}	−0.047	−0.005	−0.002	−0.002	−0.008	−0.002
$\Delta E - \Delta E_{\text{core}}$	0.008	0.003	0.003	0.000	−0.003	0.000

for an example to illustrate the evaluation. Six states in the first representation fall in the $2s$ band. A state with an energy eigenvalue of ϵ_i has a Mulliken distribution number of f_i on the central surface oxygen. The average energy of the $2s$ electron on the site of surface oxygen is defined as

$$\bar{\epsilon} = \sum_{i=1}^{6} f_i \epsilon_i \Big/ \sum_{i=1}^{6} f_i \,. \tag{7}$$

The values for the $2s$ and $2p$ electrons are tabulated in Table VI. Comparison is made between the case of the copper atom at infinity and the case of copper atom 4.0 a.u. away from the surface oxygen atom. These shifts are indicative of the size of the local effect that the adsorption of Cu has. As is evident, the largest effect occurs on the oxygen directly under the copper, and the effect is much smaller at more distant sites. As more atoms are added to the cluster, the values of the shifts $\bar{\epsilon}$ on these more remote atoms will be still smaller.

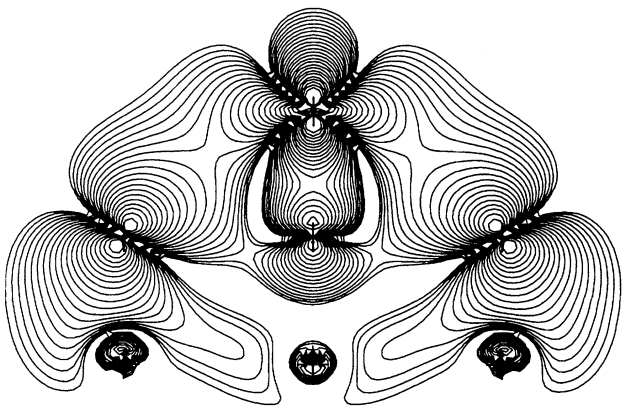

FIG. 9. This is a contour plot in the (110) plane for a state of the $3 \times 3 \times 2$ MgO cluster with the copper atom above the surface oxygen. The interaction between the Cu $3d$ and the corner O $2p$ electrons is bonding, and so is the interaction between the Cu $3d$ and the central O $2p$ electrons.

For the $2s$ band, as we have seen, it is clearly appropriate to subtract the core shifts from the shifts in $\bar{\epsilon}$. These core shifts, due to the Coulomb potential, were determined from the changes of the O $1s$ states, and are given in the second rows of Table VI. The third rows of the table gives the changes with core shifts subtracted. We have shown this subtraction even in the case of the $2p$ electrons, where its relevance is less clear, since these electrons are less localized so that the Coulomb shift will not be the same as that of a core electron. There is also no appropriate proton to cancel the effect of this shift for the $2p$ electrons, which provide the extra double minus charge to the ion. Nevertheless there is still a reasonable fall off in the subtracted numbers.

The overall conclusion is that the copper atom interacts strongly only with the oxygen atom right below it. This, together with the argument from last Sec. III B 5, tells us that the $5\times5\times2$ cluster is large enough and thick enough for this problem.

IV. DISCUSSION

Error in the local-density approximation (LDA) is something that needs discussion. First, we note that since Cu has nonzero total spin, the local spin density approximation (LSD) would be a better local approximation than the LDA. However, we made a sample calculation in the LSD with the Cu close to the equilibrium position over the oxygen site of a $3\times3\times2$ cluster, and found a difference in bonding energy of only 0.002 hartree. This was sufficiently small that it was not deemed justifiable to use the additional computational resources necessary to carry out the LSD for the larger clusters. In the discussion below, we will assume that the LSD and LDA give essentially the same result for Cu on MgO.

Although the LSD typically gives good results for small

changes within the same general environment (such as the shape of a binding energy curve near equilibrium), it tends to be poorer when two quite different environments are compared (such as would be necessary to find the depth of a binding energy curve), and the error is invariably in the direction of overbinding.[43] This error can be illustrated by results for diatomic molecules, where the LSD overbinding gets more severe when the number of electrons in the outer shells of the constituent atoms gets larger. For example, the experimental binding energy for an oxygen dimer is 5.2 eV, while LSD predicts 7.5 eV. For F_2 the LSD overbinding is even greater: the experimental binding energy is 1.65 eV, while the LSD predicts 3.4 eV. We have no way to exclude the possibility of fractional errors this large in the absolute depths of our bonding energy curves, although the shapes near equilibrium and relative depths should be much more accurate.

The LSD is typically considerably more accurate for this type of system than the Hartree Fock approximation, which typically predicts large underbinding or perhaps even negative binding. For example, it gives binding energies of 1.4 eV and −1.63 eV for the respective O_2 and F_2 dimers mentioned above. Indeed, a previous Hartree Fock calculation[31] of Cu near smaller MgO clusters than we consider here showed essentially no bonding of the Cu to the MgO.

Within the LDA, there exists a calculation[4] for Ag on MgO(001). There are similarities and differences between this calculation and ours. The main similarity is that the $4d$ and $5s$ states in Ag have roughly the same energies as the $3d$ and $4s$ states in Cu. The principal differences are (i) the outer d shell is geometrically larger in Ag and (ii) the Ag calculation was done for a metallic monolayer of Ag with the Ag atoms in one-to-one registry with either the Mg or the O substrate atoms, rather than a single Ag atom. The consequence of (i) is that the overlap of the closed O $2p$ shell and the Ag $4d$ shell forces a considerably larger equilibrium separation between the surface and Ag than what we found between the surface and Cu, thus exponentially reducing the bonding between the Ag $5s$ electron and the O $2p$ band. The consequence of (ii) and also the large equilibrium separation is that for the Ag calculation it made little difference in bonding strength whether the Ag atoms were in registry with the surface oxygens or the surface magnesiums. The value for binding of 0.3 eV per Ag atom is not grossly inconsistent with what might be obtained by extrapolating our Cu curves to a distance where they become site independent, say at a distance a little larger than 5 a.u.

That there is LDA overbinding is suggested by the combination of our results and a recent experiment. By using medium-energy ion scattering (MEIS) as an *in situ* probe of coverage,[18] Zhou, Lu, Gustafsson, and Garfunkel found that only 50% of the initially incident Cu atoms stick to the MgO(001) surface at 300 K. In their effort to explain the anomalously low sticking coefficient, they estimated the bonding strength to be a value from 0.3 to 0.5 eV. Although this precise range is dependent on the validity of the particular theoretical model they created to interpret their data, the small sticking coefficient probably does imply a shallower potential than what the LDA predicts.

Another source of error is the neglect of the copper-induced relaxation of the nuclear positions in the substrate. One would worry about the displacements of the atoms neighboring the adsorption site and about the extra depth of the potential well brought about by the relaxation of the substrate. The displacement of the oxygen atom right below the copper is expected to be small (around 0.05 a.u.), as estimated from forces on this atom when the copper was at various distances. We found the copper-induced forces on the side oxygens also to be small; by using the force constants calculated for the clean cluster,[9] we estimate the oxygen atom movement induced by these forces to be small (around 0.02 a.u.). However, the forces on the nearest magnesiums were found to be sufficiently large that the magnesium movement would be estimated to be non-negligible, and in a direction roughly parallel to the surface and away from the Cu position. This might be expected because there are no mobile electrons around the magnesium atoms to screen out the Cu-induced electric fields. The magnitude of the atomic displacements is hard to estimate. Yet we do not expect the increased well depth due to this copper induced relaxation to be substantial, since we have found that most of the binding comes from the bond between the copper atom and the oxygen right below it. Nevertheless, the effect of this relaxation would be an interesting subject for a future investigation.

Recent measurements[45] via MEIS give rather convincing evidence that Cu overlayers grow by three-dimensional islanding, even before a first layer of Cu (0.5 ML) has been deposited, although earlier experiments[11,12,15,17] had been interpreted to imply at least partial epitaxial growth. Taking the unit of area to be the area per surface O atom (~ 9 Å^2), the surface energy of Cu is[44] ~ 1 eV. This number should set a crude energy scale for the crossover between islanding and a first epitaxial layer. Our calculation predicts that the Cu well depth over an O site is also ~ 1 eV, indicating that one is close to this crossover. The lattice mismatch between the O spacing in MgO (4.2 Å) and the Cu spacing in Cu (3.6 Å) favors islanding.

Since LDA predicts the properties of occupied states correctly in many cases, we would anticipate that the results of the electronic structure from our calculations

TABLE VII. Table of the exponents α_j^μ of the Gaussians for the three types of atoms. The missing values can be obtained using the fact that the ratio $\alpha_{j+1}^\mu/\alpha_j^\mu$ is independent of j.

j	O	Mg	Cu
1	18000.0	52000.00	84100.0
2	6822.688	20591.40	34609.0
14	0.0600000	0.3061089	0.816420
15		0.1212156	0.335975
16		0.0480000	0.138261
17			0.0568977
18			0.0234147
19			0.0096357

could be found in reasonable agreement with experiment. In their electron energy loss spectroscopy study of the MgO(001) surface with small Cu coverage,[14] He and Møller found three Cu induced features (see Fig. 3 in their paper) at the positions of 2.2 eV, 4.2 eV, and $\approx$ 10 eV (the Cu induced feature around 10 eV was not numerically labeled). He and Møller gave no interpretation for the latter two peaks. In light of our calculation, it is plausible to interpret them as excitations from the antibonding and bonding states (a) and (c) of Fig. 6 to a state below the bulk band gap (see Sec. III A 2). If that is the case, the energy difference of $\approx$ 6 eV, between the two experimental features and the calculated (a) to (c) splitting of 5.8 eV, are in good agreement.

V. CONCLUSION

We conclude by restating the main LDA predictions of this paper. At the initial stages of copper adsorption, a copper atom bonds to the surface oxygen site with a bonding strength of 1.4 eV and the equilibrium distance from the surface oxygen is 1.9 Å. The copper atom could migrate over the hollow site to the next oxygen site; the diffusion barrier for this process is 0.4 eV.

ACKNOWLEDGMENTS

We thank M. Mehl and K. Jackson for discussions during the early part of this project, R. Bartynski and T. Gustafsson for discussions of the experimental aspects, and D. Vanderbilt for a thorough reading of the manuscript. The work was supported in part by the National Science Foundation Grant Nos. DMR 89-07553, DMR 91-03466, and DMR 94-07055. Computer resources were provided in part by the Pittsburgh Supercomputing Center.

APPENDIX: DESCRIPTION OF THE BASIS

A wave function in our calculations is expressed as a linear combination of wave functions centered at each atomic site. That is,

$$\psi_\lambda = \sum_\mu C_\mu \chi_\mu (\vec{r} - \vec{R}_\mu) , \tag{A1}$$

where μ labels the atomic sites. The wave function χ_μ at the site of μth atom is a linear combination of some wave functions centered at the atom, that is

$$\chi_\mu = \sum_{klm} D^\mu_{klm} \phi^\mu_{klm}(\vec{r}) , \tag{A2}$$

where $k = -1, 0, 1, \ldots, k^{\max}_\mu$ and the ranges of l and m will be given later on. The set of $\phi^\mu_{klm}(\vec{r})$ depends on μ only through the type (Cu, O, or Mg) of the μth atom and not on its position. The set of $\phi^\mu_{klm}(\vec{r})$ is the basis set for this type of atom.

TABLE VIII. Basis set for the oxygen atom. The listed quantities are the coefficients $a^{\rm O}_{klj}$ in Eq. (A4) with positive k.

j	$k=1, l=0$	$k=2, l=0$	$k=2, l=1$
1	0.36456	0.08612	−0.07596
2	0.21410	0.04934	−0.09973
3	0.56857	0.13560	−0.15257
4	0.81055	0.18917	−0.26586
5	1.3200	0.31872	−0.40752
6	1.9743	0.47867	−0.66175
7	2.5883	0.68487	−0.95832
8	2.5749	0.78550	−1.3098
9	1.3000	0.60125	−1.4275
10	0.16023	0.018669	−1.1863
11	−0.00258	−0.32980	−0.58341
12	6.96×10^{-4}	−0.19783	−0.17476
13	-1.43×10^{-4}	−0.03000	−0.02893
14	1.96×10^{-5}	5.70×10^{-5}	−0.00128

A function of the basis set of a particular type of atom is expressed in terms of some Gaussians $\mathcal{G}^\mu_j(r)$, where

$$\mathcal{G}^\mu_j(r) = e^{-\alpha^\mu_j r^2} , \tag{A3}$$

where j runs from 1 to $j^\mu_{\max}$. In our calculations, $j^\mu_{\max}$ is 14 for the oxygen atoms, 16 for the magnesium atoms, and 19 for the copper atoms. Sufficient information to obtain the evenly tempered exponents α^μ_j used in the calculation is tabulated in Table VII for the three types of the atom.

With the Gaussians, a wave function with positive k in the basis set can be written as

$$\psi^\mu_{klm}(\vec{r}) = \sum_{j=1}^{j^\mu_{\max}} a^\mu_{klj} \mathcal{G}^\mu_j(r)\, M_{l,m}(x,y,z) , \tag{A4}$$

TABLE IX. Basis set for the magnesium atom. The listed quantities are the coefficients $a^{\rm Mg}_{klj}$ in Eq. (A4) with positive k.

j	$k=1, l=0$	$k=2, l=0$	$k=3, l=0$	$k=2, l=0$
1	−0.61312	0.15538	−0.03539	−0.20091
2	−0.28293	0.07103	−0.01626	−0.33113
3	−0.89145	0.22689	−0.05161	−0.37918
4	−1.1753	0.29723	−0.06794	−0.78424
5	−1.9494	0.50071	−0.11399	−1.0580
6	−2.9043	0.75291	−0.17225	−1.8262
7	−4.1243	1.1230	−0.25672	−2.6131
8	−4.8864	1.4648	−0.33822	−3.8660
9	−3.9612	1.5219	−0.35588	−4.7635
10	−1.3404	0.78065	−0.19102	−4.8958
11	−0.06340	−0.36401	0.096489	−3.2926
12	−0.00287	−0.66492	0.21597	−1.3296
13	0.0011562	−0.23957	0.13164	−0.27826
14	-3.55×10^{-4}	−0.01114	−0.0046	−0.01810
15	8.69×10^{-5}	-3.75×10^{-4}	−0.07770	-4.36×10^{-5}
16	-1.28×10^{-5}	7.32×10^{-5}	−0.04237	-2.47×10^{-6}

TABLE X. Basis set for the copper atom. The listed quantities are the coefficients a^{Cu}_{klj} in Eq. (A4) with positive k.

j	$k=1, l=0$	$k=2, l=0$	$k=3, l=0$	$k=4, l=0$	$k=2, l=1$	$k=3, l=1$	$k=3, l=2$
1	−4.5423	1.3937	−0.53212	0.11746	−6.2022	−2.2314	15.999
2	−1.5979	0.48523	−0.18820	0.041569	−6.2373	−2.5020	−9.1168
3	−6.1659	1.9083	−0.72644	0.16035	−10.467	−3.7730	14.245
4	−7.4156	2.2939	−0.88521	0.19550	−16.495	−6.3699	2.9889
5	−11.932	3.8143	−1.4597	0.32240	−24.738	−9.1845	16.737
6	−15.897	5.3200	−2.0739	0.45862	−37.584	−14.373	17.898
7	−18.348	7.0446	−2.7765	0.61541	−52.715	−20.040	30.920
8	−13.785	6.9704	−2.9240	0.65205	−66.846	−26.276	39.640
9	−4.0725	3.1466	−1.5305	0.34809	−66.025	−26.970	49.411
10	−0.10946	−2.9804	1.3744	−0.31163	−41.491	−18.443	46.377
11	−0.02040	−3.0483	2.3846	−0.57655	−10.988	−3.4512	32.406
12	0.009285	−0.43906	0.07036	−0.01165	−0.57055	3.5224	13.375
13	5.35×10^{-4}	−0.12523	−0.61501	0.23937	−0.0043	1.8115	3.2318
14	2.89×10^{-3}	−0.07076	−0.04002	0.0959	0.00120	0.28722	0.57090
15	2.78×10^{-4}	−0.03192	0.07373	−0.04478	-2.89×10^{-4}	0.00988	0.07954
16	5.11×10^{-4}	−0.00960	0.02525	−0.087278	5.98×10^{-5}	5.78×10^{-5}	0.00817
17	1.17×10^{-4}	−0.00187	0.00577	−0.04428	-1.13×10^{-5}	-1.68×10^{-5}	3.90×10^{-4}
18	-1.21×10^{-4}	-5.41×10^{-4}	2.53×10^{-4}	−0.00393	1.82×10^{-6}	3.20×10^{-6}	3.22×10^{-6}
19	-3.18×10^{-5}	-9.19×10^{-5}	-1.09×10^{-4}	5.18×10^{-4}	-1.89×10^{-7}	-3.54×10^{-7}	2.01×10^{-8}

where $M_{lm}(x,y,z)$ are monomials in x, y, z of order l with unit coefficient. Explicitly, we have $M_{0,1}=1$, $M_{1,m}=x$, y, z, respectively, with $m=1$, 2, 3, and $M_{2,m}=x^2$, y^2, z^2, yz, zx, xy, respectively, with m from 1 to 6. The values of a^{μ}_{klj} with positive k for the three types of atom are tabulated in Table VIII, Table IX, and Table X, respectively. A positive value of k is equivalent to n, the principal quantum number labeling the principal shell of electrons of the atom; l corresponds to an angular momentum quantum number, except that for $l=2$ there is also an admixture of s states. For example, ψ_{101} is the $1s$ orbital of the atom, and ψ_{211}, ψ_{212}, and ψ_{213} are the three $2p$ orbitals. The five $3d$ orbitals can be obtained by five linear combinations of $\psi_{321},\ldots,\psi_{326}$. These orbitals are obtained from atomic calculations.

We use negative and null k values to label free Gaussians included in the basis, but which are not related to free atom wave functions. For nonpositive k, $\psi^{\mu}_{klm}(\vec{r})$ is defined as just a single Gaussian, that is

$$\psi^{\mu}_{klm}(\vec{r}) = \mathcal{G}^{\mu}_{j_{\max}+k}(r)\, M_{lm}(x,y,z)\,. \tag{A5}$$

The exponents of these two Gaussians ($k=0$ and $k=-1$) are the last two at the bottom of Table VII for each type of atom. For an O or a Mg atom, $l=0$, 1; for a Cu atom, $l=0$, 1, 2. In other words, for each type (s, p, d) of orbital of a particular atom, two long range Gaussians are included in the basis set, in addition to the fixed linear combinations of Gaussians representing atomic orbitals.

[1] K. J. Chang and M. L. Cohen, Phys. Rev. B **30**, 4774 (1984).
[2] M. J. Mehl and R. E. Cohen, J. Geophys. Res. **93**, 8009 (1988).
[3] Q. S. Wang and N. A. W. Holzwarth, Phys. Rev. B **41**, 3211 (1990).
[4] C. Li, R. Wu, A. J. Freeman, and C. L. Fu, Phys. Rev. B **48**, 8317 (1993).
[5] M. R. Pederson and K. A. Jackson, Phys. Rev. B **41**, 7453 (1990).
[6] M. Tsukada and T. Hoshino, J. Phys. Soc. Jpn. **51**, 2562 (1982).
[7] V. E. Heinrich and P. A. Cox, *The Surface of Metal Oxides* (Cambridge University, Cambridge, England, 1994).
[8] J. B. Zhou, Y. Li, H. C. Lu, D. C. Langreth, T. Gustafsson, P. Häberle, and M. R. Pederson, in *The Structure of Surfaces IV*, edited by X. D. Xie, S. Y. Tong, and M. A. van Hove (World Scientific, Singapore, 1994), p. 599.
[9] Y. Li, D. C. Langreth, and M. R. Pederson, Phys. Rev. B (to be published).
[10] J. B. Zhou, H. C. Lu, T. Gustafsson, and P. Häberle, Surf. Sci. **302**, 350 (1994).
[11] D. J. Lord and M. Prutton, Thin Solid Films **21**, 341 (1974).
[12] K. Takayanagi, K. Yaki, and G. Honjo, Thin Solid Films **48**, 137 (1978).
[13] J. W. He and P. J. Møller, Surf. Sci. **178**, 934 (1986).
[14] J. W. He and P. J. Møller, Surf. Sci. **180**, 411 (1987).
[15] I. Alstup and P. J. Møller, Appl. Surf. Sci. **33/34**, 143 (1988).
[16] D. F. Cox, T. B. Fryberger, J. W. Erickson, and S. Semancik, J. Vac. Sci. Technol. A **5**, 1170 (1987).
[17] T. Conrad, J. M. Vohs, P. A. Thiry, and R. Caudano, Surf. Interface Anal. **16**, 446 (1990).
[18] J. B. Zhou, H. C. Lu, T. Gustafsson, and E. Garfunkel, Surf. Sci. Lett. **293**, L887 (1993).

[19] K. H. Johnson and S. V. Pepper, J. Appl. Phys. **53**, 6634 (1982).
[20] H. J. Fecht and H. Gleiter, Acta Metall. **33**, 557 (1985); H. J. Fecht, *ibid.* **36**, 689 (1988).
[21] G. Fuchs, M. Treilleux, and P. Thevenard, Thin Solid Films **165**, 347 (1988).
[22] R. H. Hoel, Surf. Sci. **169**, 317 (1986).
[23] V. E. Henrich, G. Dresselhaus, and H. J. Zeiger, Phys. Rev. B **22**, 4764 (1980).
[24] P. R. Underhill and T. E. Gallon, Solid State Commun. **43**, 9 (1982).
[25] P. A. Cox and A. A. Williams, Surf. Sci. **175**, L782 (1986).
[26] V. C. Lee and H. S. Wong, J. Phys. Soc. Jpn. **45**, 895 (1978).
[27] C. Satoko, M. Tsukada, and H. Adachi, J. Phys. Soc. Jpn. **45**, 1333 (1978).
[28] M. Tsukada, H. Adachi, and C. Satoko, Prog. Surf. Sci. **14**, 113 (1983).
[29] S. Russo and C. Noguera, Surf. Sci. **262**, 245 (1992).
[30] A. Gibson and R. Haydock, J. Vac. Sci. Technol. A **10**, 2361 (1992).
[31] N. C. Bacalis and A. B. Kunz, Phys. Rev. B **32**, 4857 (1985).
[32] U. Schönberger, O. K. Andersen, and M. Methfessel, Acta Metall. Mater. **40**, 51 (1992).
[33] J. R. Smith, T. Hong, and D. J. Srolovitz, Phys. Rev. Lett. **72**, 4021 (1994).
[34] J. P. LaFemina and C. B. Duke, J. Vac. Sci. Technol. A **9**, 1847 (1991).
[35] P. Hohenberg and W. Kohn, Phys. Rev. **136**, B864 (1964); W. Kohn and L. J. Sham, *ibid.* **140**, A1133 (1965).
[36] D. M. Ceperly, Phys. Rev. B **18**, 3126 (1978); D. M. Ceperly and B. J. Alder, Phys. Rev. Lett. **45**, 566 (1980).
[37] J. P. Perdew and A. Zunger, Phys. Rev. B **23**, 5048 (1981).
[38] M. R. Pederson and K. A. Jackson, Phys. Rev. B **41**, 7453 (1990).
[39] K. M. Neyman and N. Rösch, Chem. Phys. **177**, 561 (1993).
[40] D. M. Roessler and W. C. Walker, Phys. Rev. **159**, 733 (1967).
[41] L. Fiermans, R. Hoogewijs, G. de Mayer, and J. Vennik, Phys. Status Solidi A **59**, 569 (1980).
[42] J. P. Perdew and J. R. Smith, Surf. Sci. Lett. **141**, L295 (1984).
[43] A. R. Williams and V. von Barth, in *Theory of the Inhomogeneous Electron Gas*, edited by S. Lundqvist and N. H. March (Plenum, New York, 1983), p. 246.
[44] L. Z. Mezey and J. Giber, Jpn. J. Appl. Phys. **21**, 1569 (1982).
[45] J.-B. Zhou, Ph.D. dissertation, Rutgers University, 1993.